

iFlame : Interleaving Full and Linear Attention for Efficient Mesh Generation

Hanxiao Wang
CASIA, KAUST

wanghanxiao18@mails.ucas.ac.cn

Biao Zhang*
KAUST

biao.zhang@kaust.edu.sa

Weize Quan
CASIA

qweizework@gmail.com

Dong-Ming Yan
CASIA

yandongming@gmail.com

Peter Wonka
KAUST

pwonka@gmail.com

Abstract

This paper propose iFlame¹, a novel transformer-based network architecture for mesh generation. While attention-based models have demonstrated remarkable performance in mesh generation, their quadratic computational complexity limits scalability, particularly for high-resolution 3D data. Conversely, linear attention mechanisms offer lower computational costs but often struggle to capture long-range dependencies, resulting in suboptimal outcomes. To address this trade-off, we propose an interleaving autoregressive mesh generation framework that combines the efficiency of linear attention with the expressive power of full attention mechanisms. To further enhance efficiency and leverage the inherent structure of mesh representations, we integrate this interleaving approach into an hourglass architecture, which significantly boosts efficiency. Our approach reduces training time while achieving performance comparable to pure attention-based models. To improve inference efficiency, we implemented a caching algorithm that almost doubles the speed and reduces the KV cache size by seven-eighths compared to the original Transformer. We evaluate our framework on ShapeNet and Objaverse, demonstrating its ability to generate high-quality 3D meshes efficiently. Our results indicate that the proposed interleaving framework effectively balances computational efficiency and generative performance, making it a practical solution for mesh generation. The training takes only 2 days with 4 GPUs on 39k data with a maximum of 4k faces on Objaverse.

1. Introduction

3D content generation is crucial for various domains, including virtual reality, gaming, industrial design, and dig-

ital content creation. The ability to automatically generate high-quality 3D models is fundamental to these applications, enabling more immersive experiences and efficient design workflows.

3D objects can be represented in various formats, including point clouds, voxels, implicit functions, and meshes. Among these representations, triangular meshes stand out for their widespread adoption in graphics pipelines, efficient rendering capabilities, and ability to represent complex geometries with sharp features. However, generating high-quality meshes remains challenging due to their irregular structure and the requirement to maintain geometric and topological consistency.

Recent advances in deep learning have led to significant progress in mesh generation [4, 4, 18, 38, 40, 41, 43]. Most existing approaches focus on conditional generation, where meshes are created based on point clouds or reference images. While these methods can handle complex geometries, they often rely on compressed mesh representations or intermediate formats, which may not fully preserve the original mesh properties. In contrast, unconditional mesh generation, which aims to learn the underlying distribution of 3D shapes without additional inputs, has been limited to relatively simple geometries (around 800 faces) as demonstrated in works like MeshGPT [35] and MeshXL [3].

Current mesh generation network architectures rely heavily on attention layers [39], which have shown remarkable capability in capturing complex geometric relationships. However, the quadratic computational complexity of full attention with respect to sequence length poses significant scalability challenges, especially for high-resolution meshes. This limitation becomes particularly apparent when generating meshes with thousands of faces, where computational resources become a bottleneck.

Recently, there has been more interest in linear attention [20] for sequence modeling tasks, offering linear computational complexity but typically achieving lower perfor-

*Corresponding author.

¹<https://wanghanxiao123.github.io/iFa/>

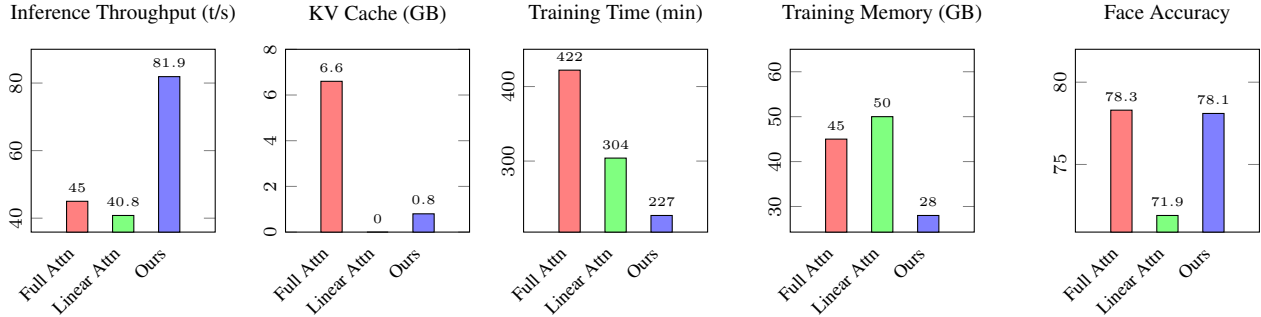


Figure 1. Performance comparison of our iFlame architecture. **(a)** Our model achieves $1.8\times$ higher inference throughput (81.9 t/s vs. 45.0 t/s). **(b)** Our model maintains low KV cache usage (0.8GB) while full attention requires $8.3\times$ more memory when generating 4000 faces. **(c, d, e)** Our model reduces training time by 46% (227 min vs. 422 min), requires 38% less GPU memory during training (28GB vs. 45GB per GPU), and maintains face accuracy (78.1% vs. 78.3%) compared to baseline methods on ShapeNet with 2B tokens.

mance compared to attention-based architectures [30]. This presents an interesting trade-off between computational efficiency and model expressiveness.

To address this trade-off, we propose an interleaving autoregressive mesh generation framework that combines the efficiency of linear attention [33] with the expressive power of full attention mechanisms [39]. By further integrating our interleaving approach into an hourglass architecture [18, 27], we achieve even greater resource efficiency. The hourglass structure enables multi-scale processing through systematic downsampling and upsampling operations, effectively capturing information at various representational scales critical for coherent mesh generation. This hierarchical design processes information at coordinate scale, vertex scale, and face scale simultaneously, allowing the model to reason about mesh geometry at different levels of abstraction. The ability to handle these interconnected spatial representations is particularly well-suited for 3D meshes, where relationships between vertices and faces must be modeled consistently across multiple scales. We evaluate our method on ShapeNet [2] and Objaverse [15], demonstrating its ability to generate high-quality 3D meshes efficiently.

As shown in Fig. 1, our model maintains comparable performance to pure attention-based models while significantly improving computational efficiency across multiple dimensions. During training of our ShapeNet [2] experiments (800 faces), our approach reduces training time requirements by **46%** and memory consumption by **38%** compared to full attention-based architectures. These efficiencies continue during inference, achieving similar token accuracy and perplexity while increasing throughput by **82%** (81.9 tokens/second vs. 45 tokens/second). Our strategy further enhances efficiency by reducing cache memory requirements by **88%** (0.8GB vs. 6.6GB) compared to standard transformer.

Thanks to the efficient Linear attention mechanisms

strategically incorporated into our design, our interleaved hourglass architecture demonstrates increasingly favorable computational characteristics as sequence length grows. This scaling efficiency enables the generation of meshes with up to 4,000 faces using limited computational resources (4 A100 GPUs)—a significant advancement over existing unconditional generation methods (also see the table for training GPU days on Objaverse).

Our comprehensive results indicate that the proposed **iFlame** framework effectively balances computational efficiency and generative performance, making it a practical solution for mesh generation tasks.

The main contributions of this work are:

- A novel interleaved hourglass architecture that strategically combines full and linear attention mechanisms, achieving high-quality mesh generation while maintaining accuracy comparable to pure attention models
- Significant efficiency gains in inference speed ($1.8\times$ faster) and cache usage (88% reduction)
- Successful scaling of unconditional mesh generation to substantially higher resolution (up to 4,000 faces) than previously possible with comparable computational resources

2. Related Work

2.1. 3D Shape Representation and Generation

Various representations have been developed for 3D shape generation, each with distinct advantages and limitations. Point cloud-based methods [1, 6, 16, 23, 47, 52] represent shapes as unordered sets of 3D points, offering simplicity but often lacking surface connectivity. Voxel-based approaches [9, 25, 44, 45] discretize 3D space into regular grids, providing explicit volumetric representations at the

	GPU Days	# Faces
M.XL [3]	968	800
M.Any [4]	32	800
M.Any v2 [5]	96	1600
E.R. [38]	560	4000
Ours	8	4000

cost of resolution limitations due to memory constraints.

Implicit function representations such as Signed Distance Functions (SDFs) [7, 28, 48, 51] and occupancy networks [24, 49, 50] encode shapes as continuous functions, enabling high-resolution surface extraction but requiring post-processing to obtain explicit geometry.

The field of autoregressive mesh generation has seen significant advancement in recent years. PolyGen [26] pioneered the approach of separately generating points and faces in an autoregressive manner to construct 3D meshes. MeshGPT [35] marked a breakthrough by introducing a unified token-based autoregressive framework for mesh generation, achieving impressive results. This was followed by Mesh Anything [4, 5], which extended the paradigm to conditional mesh generation.

MeshXL [3] demonstrated the scalability of autoregressive mesh generation on the large-scale Objaverse dataset [15]. Llama-Mesh [41] successfully explored unifying 3D mesh generation with language models, bridging the gap between NLP and geometric modeling. Research on improving token efficiency has progressed with PivotMesh [42], which explored token length compression techniques. EdgeRunner [38] employed classical mesh processing algorithms to further compress sequence length, while Weng et al. [43] and Nautilus [40] optimized mesh point indexing methods to achieve better compression ratios. MeshTron [18] leveraged an hourglass transformer architecture to improve efficiency, demonstrating excellent results for point cloud to mesh conversion. While most prior work has focused on conditional generation or sequence compression techniques, the area of high-resolution unconditional mesh generation remains relatively unexplored. To date, only MeshGPT [35] and MeshXL [3] have demonstrated the ability to generate meshes with approximately 800 faces without conditioning. This represents an important research direction worthy of further exploration. Our work advances the state-of-the-art by increasing this limit to 4,000 faces.

2.2. Linear and Hybrid Attention Mechanisms

Transformer architectures have revolutionized sequence modeling across domains, but their quadratic computational complexity with respect to sequence length creates significant scaling challenges. This limitation has catalyzed extensive research into more computationally efficient alternatives that preserve modeling capabilities.

Linear attention mechanisms fundamentally reformulate the attention operation to achieve linear complexity with sequence length. Performer [8] extended this approach by approximating the softmax kernel using random feature projections, while Cosformer [31] introduced a position-aware cosine similarity-based attention mechanism. Despite these innovations, linear attention models often struggle

with the expressivity-efficiency trade-off, as analyzed by Qin et al. [30] in their examination of the limitations inherent to linear formulations.

An alternative approach leverages recurrent architectures with enhanced expressivity. Mamba [17] introduced selective state space modeling (S4) for efficient sequence processing, achieving linear complexity while maintaining competitive performance. Its successor, Mamba2 [12], incorporates a gated update mechanism that further improves performance on language modeling and long-context understanding tasks. Similarly, RWKV [29] combines RNN-like computation with transformer-like expressivity to achieve efficient inference.

More sophisticated hybrid designs include Griffin [14], which interleaves gated linear attention with local attention patterns, and Samba [34], which integrates state space models with standard attention layers. DeltaNet [46] employs selective memory updates based on the delta rule, demonstrating particularly strong results for in-context retrieval task

Minimax-text-1 [21] pioneered the implementation of an interleaving attention structure in large language models, demonstrating the scalability and effectiveness of this architectural approach. Our work further enhances the efficiency of the interleaving strategy. While many recent approaches have introduced complex gating mechanisms or specialized activation functions to improve performance, our design philosophy emphasizes architectural simplicity and computational efficiency.

3. Method

We first describe our mesh representation, then recall the formulation of attention and linear attention before introducing our proposed iFlame architecture.

3.1. Mesh Representation

We conceptualize mesh generation as an autoregressive sequence generation problem, like MeshGPT, Meshtron and others. A triangular mesh $\mathcal{M} = (\mathcal{V}, \mathcal{F})$ has vertices $\mathcal{V} = \{\mathbf{v}^i \in \mathbb{R}^3\}_{i=1, \dots, M}$ and faces $\mathcal{F} \subset \mathcal{V} \times \mathcal{V} \times \mathcal{V}$. The number of vertices is $|\mathcal{V}| = M$ and the number of faces is $|\mathcal{F}| = N$.

To facilitate autoregressive generation, a commonly used approach (e.g., [35]) is to flatten mesh vertices \mathcal{V} into an ordered sequence by adopting a consistent convention. For example, the sequence is ordered by their z -coordinate, then by y -coordinate, and finally by x -coordinate, all in ascending order. We still use the symbol \mathcal{M} to denote the flattened sequence to simplify notation. The sequence is also augmented with special tokens: start token [S], end token [E], and padding token [P].

To allow autoregressive sampling, vertex coordinates are often quantized into 128 bins, balancing geometric precision and computational efficiency. This representation al-

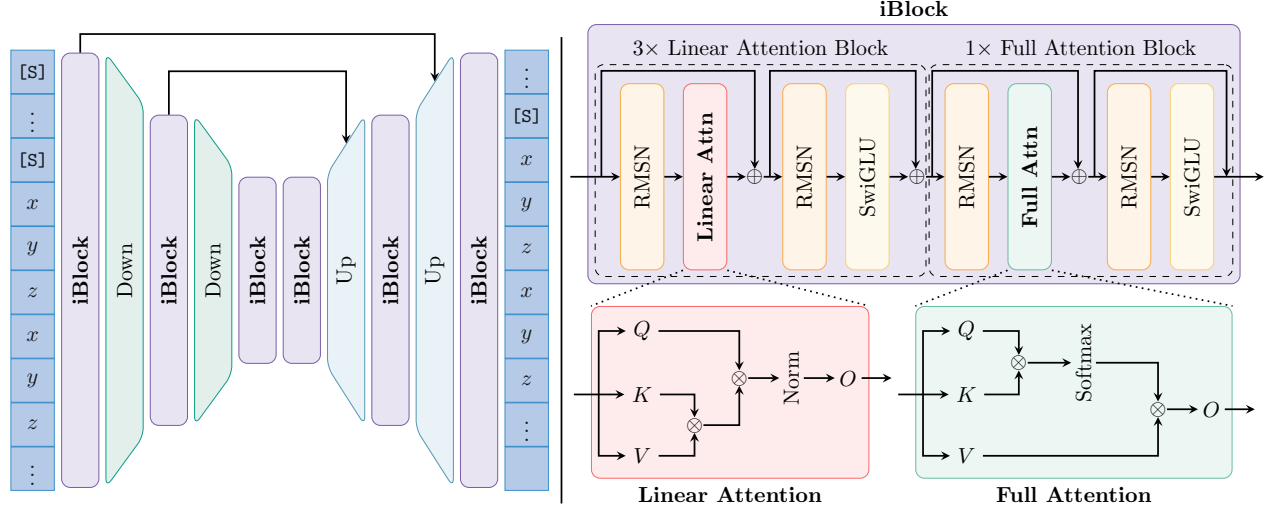


Figure 2. The architecture of our iFlame

lows us to model the mesh generation process as: $p(\mathcal{M}) = \prod_t p(q_t \mid \mathbf{q}_{<t})$ where q_t denotes each quantized coordinate value in the sequence and t means the position in the sequence.

However, this serialization approach faces significant challenges when scaling to complex meshes. When flattened into a sequence, a mesh with N faces results in a sequence of length $9N$ (3 vertices per face, each with 3 coordinates). Standard transformer (with full attention) architectures with context lengths of 4096 or 8192 tokens can only process a limited number of faces. Existing methods struggle to scale efficiently due to the quadratic complexity of attention mechanisms, which are both time and memory-intensive. While Messtron attempts to address this by using truncated sequences during training, experiments from [43] show that this approach often leads to discontinuities in the generated meshes.

To address these scaling challenges, we first revisit the fundamental attention mechanisms that underlie transformer architectures. Full attention offers strong expressiveness but lacks efficiency, while linear attention provides efficiency at the cost of effectiveness. This insight motivates our interleaving approach.

3.2. Preliminary

Attention. The original transformer design [39] utilizes a self-attention mechanism that can be mathematically represented as:

$$\text{Softmax}\left(QK^\top/\sqrt{d}\right)V \quad (1)$$

In this formulation, Q , K , and $V \in \mathbb{R}^{n \times d}$ represent the query, key, and value matrices, respectively, where n refers to the sequence length and d indicates the feature dimensionality. The computational burden of this approach arises from calculating the full attention matrix $QK^\top \in \mathbb{R}^{n \times n}$,

resulting in $O(n^2d)$ complexity during training. Flash Attention [10, 13] significantly improves the efficiency of computing this operation through careful memory management, without changing the mathematical formulation. For autoregressive generation tasks, when producing the m -th token, the model requires $O(md^2)$ computations as it must attend to all previously generated tokens.

Linear Attention. As an alternative, linear attention variants like Lightning attention [32] reformulate the attention mechanism by removing the computationally intensive softmax and scaling operations. This approach can be expressed as:

$$\text{Norm}((QK^\top)V) \quad (2)$$

To achieve better computational efficiency, this expression can be algebraically rearranged into its equivalent linear form:

$$\text{Norm}(Q(K^\top V)) \quad (3)$$

This rearrangement significantly improves efficiency by reducing the computational complexity to $O(nd^2)$ during the training phase, with benefits becoming more pronounced as sequence length increases. During inference, linear attention maintains a consistent $O(d^2)$ computational complexity regardless of context length by progressively updating the $K^\top V$ term, enabling efficient processing of sequences of any practical length.

3.3. Interleaving Attention Block

After analyzing the trade-offs between full and linear attention, it is natural to conjecture that an interleaving approach can significantly reduce computational costs while maintaining model expressiveness. This insight led us to design an interleaving block architecture that strategically combines both attention mechanisms.

Minimax-text-1 [21] was the first large language model to implement an interleaving attention structure. However, like other modern linear attention implementations, their approach often employs KQV SiLU and gate mechanisms, which consume substantial computational resources. To enhance efficiency and maintain structural symmetry with full attention, we adopt a minimalist linear attention design, referred to as **simplified linear attention**, as illustrated in our pipeline (Fig. 2).

Each transformer block consists of a self-attention layer followed by a feed-forward network, both equipped with residual connections and pre-normalization layers. Given an input sequence $X \in \mathbb{R}^{n \times d}$, the block computations are formulated as:

$$\begin{aligned} X &\leftarrow X + f(\text{RMSNorm}(X)) \\ Y &\leftarrow X + \text{SwiGLU}(\text{RMSNorm}(X)) \end{aligned} \quad (4)$$

The attention function f can adaptively switch between the full attention mechanism in Equation (1) and the linear attention variant in Equation (3). For causal attention, appropriate masking is applied to ensure that each position can only attend to previous positions. Additionally, Rotary Position Embeddings (RoPE [36]) are incorporated into the computation of Q and K to encode positional information.

3.4. Hourglass Structure

Building upon our interleaving attention blocks, we further enhance efficiency by leveraging the inherent hierarchical structure of meshes. The natural face-vertex-coordinate structure of meshes is particularly well-suited for an hourglass network architecture like Meshtron, which can substantially reduce computational demands.

The Hourglass structure operates across three scales through six interconnected blocks. The first block encodes coordinates to extract fine-grained features (Φ_{coord}), which are downsampled to vertex features for the second block. This vertex encoder returns vertex feature (Φ_{vertex}), further downsamples to produce face features for the network core (blocks three and four). To maintain causality, face features, which includes all vertex data, cannot be directly fused with the points in a face. Instead, a shifting mechanism is used; for example, with three points defining a face, a shift of 2 ensures that only the last point receives complete face information. The face features are combined with shifted vertex features (Φ_{vertex}) from the second block and processed through the fifth block. After upsampling to Ψ_{coord} , these features are integrated with the shifted coordinate features (Φ_{coord}) and processed by the final block to produce the output. This multi-scale architecture enables efficient feature extraction and integration, enhancing mesh processing capabilities.

3.5. Inference

The hourglass architecture naturally processes information at multiple scales through its downsampling and upsampling operations. Implementing this hierarchical approach for efficient inference requires careful design to manage the complex token dependencies and state tracking across different resolution levels.

We designed an inference algorithm that respects these architectural constraints while minimizing unnecessary computation. In our method, the base encoder and final decoder process every token, the intermediate layers process every third token, and the bottleneck layers handle every ninth token. This hierarchical approach necessitates maintaining circular buffers to effectively track states across different resolution levels.

The key efficiency of our approach comes from the strategic integration of three linear attention layers and one full attention layer in our **iBlock**. The linear layers require $O(1)$ key-value cache, while full attention requires $O(n)$, enabling a 75% reduction in cache memory usage. Furthermore, the hourglass structure further decreases the cache consumption, resulting in an overall reduction of over 87% compared to full attention. Our implementation leverages a multi-resolution processing pipeline and the low cache property of **iBlock**, allowing the system to capture dependencies at various temporal scales while maintaining manageable computational and memory requirements.

4. Experimental Setup

4.1. Implementation Details

For ShapeNet, we train a 24-layer transformer (76M parameters) with embedding dimension 512 and 16 attention heads. We use 4 A100 GPUs with batch size 64, Muon [19, 22] optimizer with 1×10^{-3} learning rate, 2-epoch warmup and cosine decay. For Objaverse, we scale to a 24-layer transformer (0.3B parameters) with embedding dimension 1024 and 16 attention heads. Training uses 4 A100 GPUs with batch size 16, for 2 days. Muon optimizer with 3×10^{-4} learning rate, following the same warmup and decay schedule. To optimize memory usage and computational efficiency, we employ Flash Attention 2 [11] for full attention computation and Lightning Attention [32] for linear attention operations.

We set up the baseline as follows: full attention, linear attention, interleaving full and linear attention (**I**), interleaving full and simplified linear attention (**I+S**), interleaving full and simplified linear attention with hourglass architecture (**I+S+H**). For inference, we employ nucleus sampling with top-p value of 0.95 and top-k value of 50, which provides a good balance between diversity and quality in the generated meshes.

4.2. Data Processing and Augmentation

Following the MeshGPT preprocessing pipeline, we filter the ShapeNet dataset to include meshes with fewer than 800 faces, resulting in 28,570 meshes for training and 430 for testing. We utilize the training subset provided by [37]. We then filter out meshes with more than 4,000 faces, yielding 39,232 meshes for training and 4,368 for testing. During training, we employ random scaling and random translation.

5. Result

5.1. Training Phase

Table 1 demonstrates the significant efficiency advantages of our approach during training on ShapeNet dataset. The simplified interleaving architecture (**I+S**) reduces per-GPU memory consumption from 63GB to 51GB, a 20% reduction compared to the original interleaving architecture (**I**), while decreasing training time from 5 hours and 41 minutes to 5 hours and 24 minutes (5.0% improvement).

While the full attention model achieves relatively low peak memory usage (45GB/GPU)² due to extensive optimizations in flash attention implementations, it requires 30% longer training time than **I+S** (7 hours and 2 minutes vs. 5 hours and 24 minutes).

Our full architecture (**I+S+H**), which incorporates both simplified interleaving and the hourglass structure, delivers substantially greater improvements across all metrics. It reduces memory requirements to just 28GB per GPU (a 56% reduction compared to **I** and 38% compared to full attention) while completing training in only 3 hours and 47 minutes—a 30% reduction in training time versus **I+S** and 46% versus full attention. These dramatic efficiency gains make high-quality mesh generation more accessible even with limited computational resources.

Architecture	Memory	Epochs	Time
Full Attn	45G×4	40	7h 02m
Linear Attn	50G×4	40	5h 04m
I	63G×4	40	5h 41m
I+S	51G×4	40	5h 24m
I+S+H (Ours)	28G×4	40	3h 47m

Table 1. Resource usage comparison (4 GPUs).

5.2. Inference Phase

This section analyzes inference performance across five model variants, with a batch size of 4 and 36000 tokens (4000 faces × 9 vertices). Standard interleaving (**I**) exhibits

²Flash attention can achieve linear memory complexity, but the time complexity remains quadratic.

the highest latency (25.7 ms/token) due to SiLU activations and gate mechanisms, while our simplified version (**I+S**) demonstrates improved efficiency. Our complete architecture (**I+S+H**) achieves the lowest latency (12.2 ms/token) and fastest processing time (439.2 seconds), representing a 45% improvement over the most efficient baseline.

Regarding memory consumption, full attention models use significantly more memory, while linear attention models use the least. Our interleaving approaches consume similar amounts of memory, offering a trade-off between computational efficiency and model expressiveness.

Metric	Full Attn	Linear Attn	I	I+S	I+S+H (Ours)
Latency (ms/t)	22.2	24.5	25.7	24.3	12.2
Throughput (t/s)	45.0	40.8	38.9	41.1	81.9
GPU (GB)	9.5	2.9	3.7	3.7	3.7
KV Cache (GB)	6.6	0.0	0.8	0.8	0.8
Total Time (s)	800.6	881.2	925.3	874.7	439.2

Table 2. Inference performance comparison.

5.3. Generation Quality Metrics

Table 3 compares performance across different models and categories. For Token Accuracy, **I**, **I+S** and **I+S+H** achieve 96.3%, matching **I** and only 0.2% below full attention, while linear attention achieves 95.2%. In Face Accuracy, **I+S+H** performs best among our proposed variants at 78.1%, nearly matching full attention’s 78.3%, with **I+S** and **I** achieving 77.2% and 77.8% respectively. Linear attention lags significantly at 71.9%. For Perplexity, full attention, **I**, and **I+S** all achieve 1.14, with **I+S+H** slightly higher at 1.15 and linear attention at 1.18. These results demonstrate that our model maintains near-optimal performance while improving computational efficiency.

5.4. Qualitative Results

Figures 3 and 4 showcase the qualitative results of our proposed approach. As demonstrated in Figure 3, our model achieves mesh generation quality comparable to MeshGPT on ShapeNet while requiring significantly fewer parameters. For the more challenging Objaverse dataset, Figure 4 illustrates our model’s capability to generate complex meshes with intricate geometric details and structures.

5.5. Ablation Study

We evaluate different model architectures by testing their ability to complete mesh geometry when given the first 50 faces as input (Fig. 5). The linear attention model produces the poorest results with disconnected meshes. Full attention generates more detailed outputs due to its greater capacity. The interleaving model (**I**) and (**I+S**) show intermediate performance levels. Our approach (**I+S+H**) achieves results comparable to full attention while maintaining computational efficiency, validating our architectural design choices.

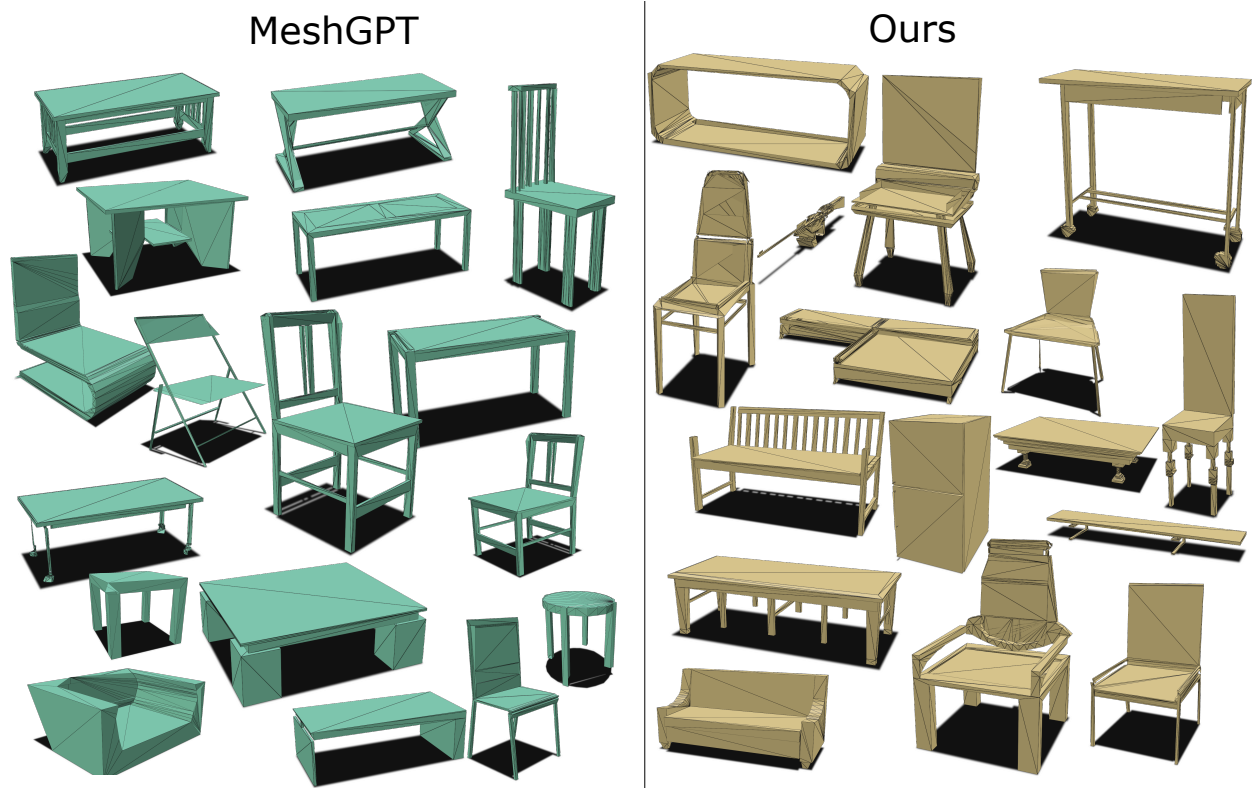


Figure 3. Comparison of 3D mesh generation quality between MeshGPT (197M parameters) and **our model iFlame (76M parameters)** on ShapeNet.

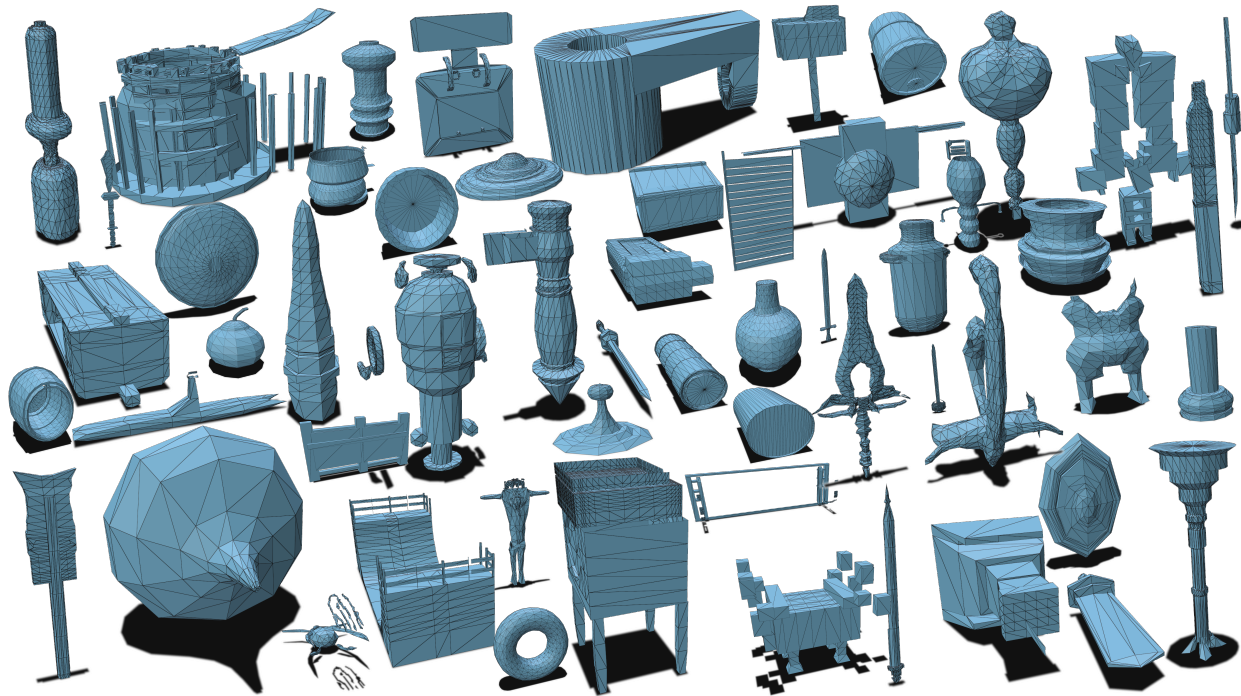


Figure 4. Generative results on Objaverse.

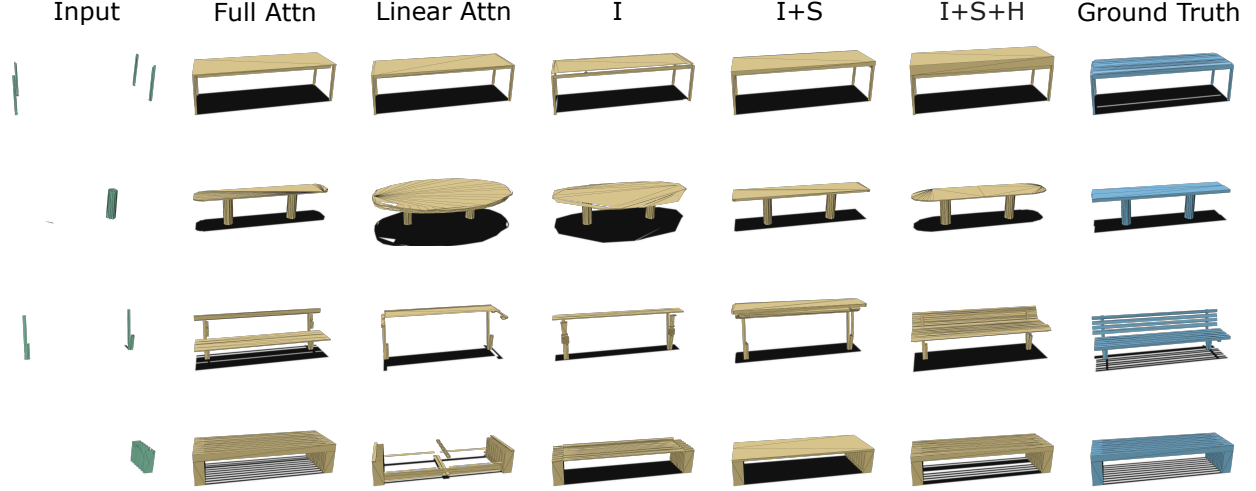


Figure 5. Ablation study on ShapeNet.

Category	Full attn	Linear attn	I	I+S	I+S+H
Token Accuracy (%) \uparrow					
Bench	96.6	95.5	96.6	96.5	96.6
Bookshelf	98.1	97.2	98.1	97.8	98.2
Chair	94.9	93.4	94.8	94.7	94.7
Display	94.9	93.2	94.7	94.6	94.7
Table	97.4	96.3	97.3	97.2	97.3
All	96.5	95.2	96.3	96.3	96.3
Face Accuracy (%) \uparrow					
Bench	78.5	72.3	78.9	77.7	79.1
Bookshelf	87.6	81.9	87.3	86.0	87.5
Chair	70.4	63.7	70.0	69.6	70.3
Display	69.0	61.9	68.2	67.4	68.0
Table	83.2	77.1	82.5	82.0	82.9
All	78.3	71.9	77.8	77.2	78.1
Perplexity (PPL) \downarrow					
Bench	1.13	1.16	1.12	1.13	1.13
Bookshelf	1.07	1.09	1.07	1.08	1.07
Chair	1.22	1.26	1.22	1.22	1.23
Display	1.21	1.26	1.21	1.21	1.21
Table	1.10	1.13	1.10	1.10	1.10
All	1.14	1.18	1.14	1.14	1.15

Table 3. Accuracy comparison across different models and categories.

5.6. Scalability

We conducted an experiment on our model’s scalability by varying the embedding dimension across three configurations: 256, 512, and 1024. Each configuration was trained for 10 epochs under identical conditions to ensure fair comparison. Figure 6 illustrates the results of these experiments.

Our results show a clear relationship between model

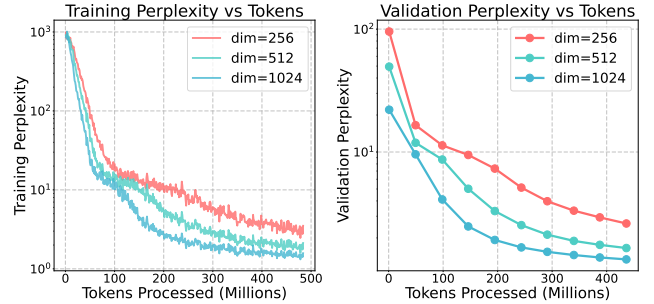


Figure 6. PPL comparison across different embedding dimension. Lower PPL indicates better performance.

size and perplexity. Increasing the embedding dimension consistently improves performance, with the 1024-dimensional model significantly outperforming the 256-dimensional version. This demonstrates that our interleaving attention mechanism effectively utilizes additional parameters without suffering from typical optimization challenges in larger models, suggesting potential for further improvements through additional scaling.

6. Conclusion and Future Work

We presented iFlame, an architecture for efficient mesh generation that balances computational efficiency with generative performance through interleaved full and linear attention mechanisms. Our approach demonstrates substantial efficiency improvements while maintaining high-quality output.

Future work includes scaling to larger meshes (10,000+ faces), increasing model capacity through larger embedding dimensions or deeper networks, exploring Mixture of Experts architectures for parameter efficiency, and extending to conditional generation scenarios such as point-to-mesh

or image-to-mesh tasks.

We believe iFlame represents a significant advancement toward making high-quality mesh generation more accessible and practical for real-world applications.

References

- [1] Panos Achlioptas, Olga Diamanti, Ioannis Mitliagkas, and Leonidas Guibas. Learning representations and generative models for 3d point clouds. In *International conference on machine learning*, pages 40–49. PMLR, 2018. 2
- [2] Angel X Chang, Thomas Funkhouser, Leonidas Guibas, Pat Hanrahan, Qixing Huang, Zimo Li, Silvio Savarese, Manolis Savva, Shuran Song, Hao Su, et al. Shapenet: An information-rich 3d model repository. *arXiv preprint arXiv:1512.03012*, 2015. 2
- [3] Sijin Chen, Xin Chen, Anqi Pang, Xianfang Zeng, Wei Cheng, Yijun Fu, Fukun Yin, Billz Wang, Jingyi Yu, Gang Yu, et al. Meshxl: Neural coordinate field for generative 3d foundation models. *Advances in Neural Information Processing Systems*, 37:97141–97166, 2025. 1, 2, 3, 13
- [4] Yiwen Chen, Tong He, Di Huang, Weicai Ye, Sijin Chen, Jiaxiang Tang, Xin Chen, Zhongang Cai, Lei Yang, Gang Yu, et al. Meshanything: Artist-created mesh generation with autoregressive transformers. *arXiv preprint arXiv:2406.10163*, 2024. 1, 2, 3, 13
- [5] Yiwen Chen, Yikai Wang, Yihao Luo, Zhengyi Wang, Zilong Chen, Jun Zhu, Chi Zhang, and Guosheng Lin. Meshanything v2: Artist-created mesh generation with adjacent mesh tokenization. *arXiv preprint arXiv:2408.02555*, 2024. 2, 3, 12, 13
- [6] An-Chieh Cheng, Xueting Li, Sifei Liu, Min Sun, and Ming-Hsuan Yang. Autoregressive 3d shape generation via canonical mapping. *arXiv preprint arXiv:2204.01955*, 2022. 2
- [7] Julian Chibane, Thiemo Alldieck, and Gerard Pons-Moll. Implicit functions in feature space for 3d shape reconstruction and completion. In *Proceedings of the IEEE/CVF Conference on Computer Vision and Pattern Recognition*, pages 6970–6981, 2020. 3
- [8] Krzysztof Marcin Choromanski, Valerii Likhoshesterov, David Dohan, Xingyou Song, Andreea Gane, Tamás Székely, Peter Hawkins, Jared Quincy Davis, Afroz Mohiuddin, Lukasz Kaiser, David Benjamin Belanger, Lucy J. Colwell, and Adrian Weller. Rethinking attention with performers. In *9th International Conference on Learning Representations, ICLR 2021, Virtual Event, Austria, May 3-7, 2021*. OpenReview.net, 2021. 3
- [9] Christopher Bongo Choy, Danfei Xu, JunYoung Gwak, Kevin Chen, and Silvio Savarese. 3d-r2n2: A unified approach for single and multi-view 3d object reconstruction. *European conference on computer vision*, pages 628–644, 2016. 2
- [10] Tri Dao. Flashattention-2: Faster attention with better parallelism and work partitioning. *arXiv preprint arXiv:2307.08691*, 2023. 4
- [11] Tri Dao. Flashattention-2: Faster attention with better parallelism and work partitioning. *ArXiv preprint, abs/2307.08691*, 2023. 5
- [12] Tri Dao and Albert Gu. Transformers are ssms: Generalized models and efficient algorithms through structured state space duality. *arXiv preprint arXiv: 2405.21060*, 2024. 3
- [13] Tri Dao, Dan Fu, Stefano Ermon, Atri Rudra, and Christopher Ré. Flashattention: Fast and memory-efficient exact attention with io-awareness. *Advances in neural information processing systems*, 35:16344–16359, 2022. 4
- [14] Soham De, Samuel L. Smith, Anushan Fernando, Aleksandar Botev, George Cristian-Muraru, Albert Gu, Ruba Haroun, Leonard Berrada, Yutian Chen, Srivatsan Srinivasan, Guillaume Desjardins, Arnaud Doucet, David Budden, Yee Whye Teh, Razvan Pascanu, Nando De Freitas, and Caglar Gulcehre. Griffin: Mixing Gated Linear Recurrences with Local Attention for Efficient Language Models, 2024. 3
- [15] Matt Deitke, Dustin Schwenk, Jordi Salvador, Luca Weihs, Oscar Michel, Eli VanderBilt, Ludwig Schmidt, Kiana Ehsani, Aniruddha Kembhavi, and Ali Farhadi. Objaverse: A universe of annotated 3d objects. In *Proceedings of the IEEE/CVF conference on computer vision and pattern recognition*, pages 13142–13153, 2023. 2, 3
- [16] Haoqiang Fan, Hao Su, and Leonidas J. Guibas. A point set generation network for 3d object reconstruction from a single image. In *2017 IEEE Conference on Computer Vision and Pattern Recognition (CVPR)*, pages 2463–2471, 2017. 2
- [17] Albert Gu and Tri Dao. Mamba: Linear-time sequence modeling with selective state spaces. 2023. 3
- [18] Zekun Hao, David W Romero, Tsung-Yi Lin, and Ming-Yu Liu. Meshtron: High-fidelity, artist-like 3d mesh generation at scale. *arXiv preprint arXiv:2412.09548*, 2024. 1, 2, 3, 13
- [19] Keller Jordan et al. Muon: An optimizer for hidden layers in neural networks, 2024. 5
- [20] Angelos Katharopoulos, Apoorv Vyas, Nikolaos Pappas, and François Fleuret. Transformers are rnns: Fast autoregressive transformers with linear attention. In *Proceedings of the 37th International Conference on Machine Learning, ICML 2020, 13-18 July 2020, Virtual Event*, pages 5156–5165. PMLR, 2020. 1
- [21] Aonian Li, Bangwei Gong, Bo Yang, Boji Shan, Chang Liu, Cheng Zhu, Chunhao Zhang, Congchao Guo, Da Chen, Dong Li, et al. Minimax-01: Scaling foundation models with lightning attention. *arXiv preprint arXiv:2501.08313*, 2025. 3, 5
- [22] Jingyuan Liu, Jianlin Su, Xingcheng Yao, Zhejun Jiang, Guokun Lai, Yulun Du, Yidao Qin, Weixin Xu, Enzhe Lu, Junjie Yan, et al. Muon is scalable for llm training. *arXiv preprint arXiv:2502.16982*, 2025. 5
- [23] Shitong Luo and Wei Hu. Diffusion probabilistic models for 3d point cloud generation. In *Proceedings of the IEEE/CVF Conference on Computer Vision and Pattern Recognition*, pages 2837–2845, 2021. 2
- [24] Lars Mescheder, Michael Oechsle, Michael Niemeyer, Sebastian Nowozin, and Andreas Geiger. Occupancy networks: Learning 3d reconstruction in function space. In *Proceedings of the IEEE/CVF conference on computer vision and pattern recognition*, pages 4460–4470, 2019. 3

- [25] Paritosh Mittal, Yen-Chi Cheng, Maneesh Singh, and Shubham Tulsiani. Autosdf: Shape priors for 3d completion, reconstruction and generation. In *Proceedings of the IEEE/CVF Conference on Computer Vision and Pattern Recognition*, pages 306–315, 2022. 2
- [26] Charlie Nash, Yaroslav Ganin, SM Ali Eslami, and Peter Battaglia. Polygen: An autoregressive generative model of 3d meshes. In *International conference on machine learning*, pages 7220–7229. PMLR, 2020. 3
- [27] Piotr Nawrot, Szymon Tworkowski, Michał Tyrolski, Łukasz Kaiser, Yuhuai Wu, Christian Szegedy, and Henryk Michalewski. Hierarchical transformers are more efficient language models. *arXiv preprint arXiv:2110.13711*, 2021. 2
- [28] Jeong Joon Park, Peter Florence, Julian Straub, Richard Newcombe, and Steven Lovegrove. Deepsdf: Learning continuous signed distance functions for shape representation. In *Proceedings of the IEEE/CVF conference on computer vision and pattern recognition*, pages 165–174, 2019. 3
- [29] Bo Peng, Eric Alcaide, Quentin Anthony, Alon Albalak, Samuel Arcadinho, Stella Biderman, Huanqi Cao, Xin Cheng, Michael Chung, Leon Derczynski, Xingjian Du, Matteo Grella, Kranthi Gv, Xuzheng He, Haowen Hou, Przemysław Kazienko, Jan Kocon, Jiaming Kong, Bartłomiej Koptyra, Hayden Lau, Jiaju Lin, Krishna Sri Ipsit Mantri, Ferdinand Mom, Atsushi Saito, Guangyu Song, Xiangru Tang, Johan Wind, Stanisław Woźniak, Zhenyuan Zhang, Qinghua Zhou, Jian Zhu, and Rui-Jie Zhu. RWKV: Reinventing RNNs for the transformer era. In *Findings of the Association for Computational Linguistics: EMNLP 2023*, pages 14048–14077, Singapore, 2023. Association for Computational Linguistics. 3
- [30] Zhen Qin, Xiaodong Han, Weixuan Sun, Dongxu Li, Lingpeng Kong, Nick Barnes, and Yiran Zhong. The devil in linear transformer. In *Proceedings of the 2022 Conference on Empirical Methods in Natural Language Processing*, pages 7025–7041, Abu Dhabi, United Arab Emirates, 2022. Association for Computational Linguistics. 2, 3
- [31] Zhen Qin, Weixuan Sun, Hui Deng, Dongxu Li, Yunshen Wei, Baohong Lv, Junjie Yan, Lingpeng Kong, and Yiran Zhong. cosformer: Rethinking softmax in attention. In *The Tenth International Conference on Learning Representations, ICLR 2022, Virtual Event, April 25-29, 2022*. OpenReview.net, 2022. 3
- [32] Zhen Qin, Weigao Sun, Dong Li, Xuyang Shen, Weixuan Sun, and Yiran Zhong. Lightning attention-2: A free lunch for handling unlimited sequence lengths in large language models. 2024. 4, 5
- [33] Zhen Qin, Weigao Sun, Dong Li, Xuyang Shen, Weixuan Sun, and Yiran Zhong. Lightning attention-2: A free lunch for handling unlimited sequence lengths in large language models. *ArXiv preprint*, abs/2401.04658, 2024. 2
- [34] Liliang Ren, Yang Liu, Yadong Lu, Yelong Shen, Chen Liang, and Weizhu Chen. Samba: Simple hybrid state space models for efficient unlimited context language modeling. *ArXiv preprint*, abs/2406.07522, 2024. 3
- [35] Yawar Siddiqui, Antonio Alliegro, Alexey Artemov, Tatiana Tommasi, Daniele Sirigatti, Vladislav Rosov, Angela Dai, and Matthias Nießner. Meshgpt: Generating triangle meshes with decoder-only transformers. In *Proceedings of the IEEE/CVF conference on computer vision and pattern recognition*, pages 19615–19625, 2024. 1, 3, 13
- [36] Jianlin Su, Yu Lu, Shengfeng Pan, Bo Wen, and Yunfeng Liu. Roformer: Enhanced transformer with rotary position embedding. *ArXiv preprint*, abs/2104.09864, 2021. 5
- [37] Jiaxiang Tang, Zhaoxi Chen, Xiaokang Chen, Tengfei Wang, Gang Zeng, and Ziwei Liu. Lgm: Large multi-view gaussian model for high-resolution 3d content creation. In *European Conference on Computer Vision*, pages 1–18. Springer, 2024. 6
- [38] Jiaxiang Tang, Zhaoshuo Li, Zekun Hao, Xian Liu, Gang Zeng, Ming-Yu Liu, and Qinsheng Zhang. Edgerunner: Auto-regressive auto-encoder for artistic mesh generation. *arXiv preprint arXiv:2409.18114*, 2024. 1, 2, 3, 13
- [39] Ashish Vaswani, Noam Shazeer, Niki Parmar, Jakob Uszkoreit, Llion Jones, Aidan N Gomez, Łukasz Kaiser, and Illia Polosukhin. Attention is all you need. *Advances in neural information processing systems*, 30, 2017. 1, 2, 4
- [40] Yuxuan Wang, Xuanyu Yi, Haohan Weng, Qingshan Xu, Xiaokang Wei, Xianghui Yang, Chunchao Guo, Long Chen, and Hanwang Zhang. Nautilus: Locality-aware auto-encoder for scalable mesh generation. *arXiv preprint arXiv:2501.14317*, 2025. 1, 3
- [41] Zhengyi Wang, Jonathan Lorraine, Yikai Wang, Hang Su, Jun Zhu, Sanja Fidler, and Xiaohui Zeng. Llama-mesh: Unifying 3d mesh generation with language models. *arXiv preprint arXiv:2411.09595*, 2024. 1, 3
- [42] Haohan Weng, Yikai Wang, Tong Zhang, CL Chen, and Jun Zhu. Pivotmesh: Generic 3d mesh generation via pivot vertices guidance. *arXiv preprint arXiv:2405.16890*, 2024. 3, 13
- [43] Haohan Weng, Zibo Zhao, Biwen Lei, Xianghui Yang, Jian Liu, Zeqiang Lai, Zhuo Chen, Yuhong Liu, Jie Jiang, Chunchao Guo, et al. Scaling mesh generation via compressive tokenization. *arXiv preprint arXiv:2411.07025*, 2024. 1, 3, 4, 12, 13
- [44] Zhirong Wu, Shuran Song, Aditya Khosla, Fisher Yu, Linguang Zhang, Xiaoou Tang, and Jianxiong Xiao. 3d shapenets: A deep representation for volumetric shapes. In *Proceedings of the IEEE conference on computer vision and pattern recognition*, pages 1912–1920, 2015. 2
- [45] Jianwen Xie, Zilong Zheng, Ruiqi Gao, Wenguan Wang, Song-Chun Zhu, and Ying Nian Wu. Generative voxelnet: learning energy-based models for 3d shape synthesis and analysis. *IEEE Transactions on Pattern Analysis and Machine Intelligence*, 2020. 2
- [46] Songlin Yang, Bailin Wang, Yu Zhang, Yikang Shen, and Yoon Kim. Parallelizing linear transformers with the delta rule over sequence length. *NeurIPS*, 2024. 3
- [47] Xiaohui Zeng, Arash Vahdat, Francis Williams, Zan Gojcic, Or Litany, Sanja Fidler, and Karsten Kreis. Lion: Latent point diffusion models for 3d shape generation. *arXiv preprint arXiv:2210.06978*, 2022. 2
- [48] Biao Zhang and Peter Wonka. Functional diffusion. In *Proceedings of the IEEE/CVF Conference on Computer Vision and Pattern Recognition*, pages 4723–4732, 2024. 3

- [49] Biao Zhang and Peter Wonka. Lagem: A large geometry model for 3d representation learning and diffusion. *arXiv preprint arXiv:2410.01295*, 2024. [3](#)
- [50] Biao Zhang, Jiapeng Tang, Matthias Niessner, and Peter Wonka. 3DShape2VecSet: A 3d shape representation for neural fields and generative diffusion models. *ACM Transactions On Graphics (TOG)*, 42(4):1–16, 2023. [3](#)
- [51] Xin-Yang Zheng, Yang Liu, Peng-Shuai Wang, and Xin Tong. Sdf-stylegan: Implicit sdf-based stylegan for 3d shape generation. In *Comput. Graph. Forum (SGP)*, 2022. [3](#)
- [52] Linqi Zhou, Yilun Du, and Jiajun Wu. 3d shape generation and completion through point-voxel diffusion. In *Proceedings of the IEEE/CVF International Conference on Computer Vision*, pages 5826–5835, 2021. [2](#)

A. Appendix

This section details iFlame’s efficient token processing techniques, focusing on Selective Cache-Efficient Token Processing (Algorithm 2) and Interleaving Attention Processing (Algorithm 1). These algorithms enhance computational efficiency and memory usage during inference while preserving output quality. Through optimized caching and selective computation, iFlame handles longer sequences with limited resources. Additional generated results from the Objaverse dataset are presented in Figures 1, 2, and 3. Table 1 compares recent mesh generation approaches. Mesh sequence length remains a fundamental challenge, with researchers typically pursuing either: (1) autoencoder compression to represent faces with fewer tokens, or (2) sequence-compressing serialization methods. However, we focused on the architectural design for mesh generation. We can further incorporate other designs (*e.g.*, the sequence ordering [5, 43]) to improve the performance.

Algorithm 1 Interleaving Attention Processing in iBlock with Selective Caching

Require: \mathbf{x}_t : Input embedding at position t
Require: \mathcal{C} : Key-value cache state
Ensure: \mathbf{y}_t : Processed representation

```

1: function INTERLEAVINGATTENTIONBLOCK( $\mathbf{x}_t, t$ )
2:    $\mathbf{x}'_t \leftarrow \text{LayerNorm}(\mathbf{x}_t)$   $\triangleright$  Pre-normalization
3:    $\mathbf{q}_t, \mathbf{k}_t, \mathbf{v}_t \leftarrow \text{ProjectQKV}(\mathbf{x}'_t)$ 
4:    $\mathbf{q}_t, \mathbf{k}_t \leftarrow \text{ApplyRotaryEmbedding}(\mathbf{q}_t, \mathbf{k}_t, t)$   $\triangleright$ 
      Position encoding
5:   if  $t \bmod 4 = 0$  then  $\triangleright$  Full attention
6:      $\mathcal{C}.\text{KV}[:, t \bmod L] \leftarrow (\mathbf{k}_t, \mathbf{v}_t)$ 
7:      $\mathbf{a}_t \leftarrow \text{FullAttention}(\mathbf{q}_t, \mathcal{C}.\text{KV})$ 
8:   else  $\triangleright$  Linear attention
9:      $\mathcal{C}.\text{State} \leftarrow \text{UpdateState}(\mathcal{C}.\text{State}, \mathbf{k}_t, \mathbf{v}_t)$ 
10:     $\mathbf{a}_t \leftarrow \text{LinearAttention}(\mathbf{q}_t, \mathcal{C}.\text{State})$ 
11:   end if
12:    $\mathbf{z}_t \leftarrow \mathbf{x}_t + \mathbf{a}_t$   $\triangleright$  First residual connection
13:    $\mathbf{z}'_t \leftarrow \text{LayerNorm}(\mathbf{z}_t)$   $\triangleright$  Second normalization
14:    $\mathbf{f}_t \leftarrow \text{FeedForward}(\mathbf{z}'_t)$   $\triangleright$  Position-wise FFN
15:    $\mathbf{y}_t \leftarrow \mathbf{z}_t + \mathbf{f}_t$   $\triangleright$  Second residual connection
16:   return  $\mathbf{y}_t$ 
17: end function

```

Algorithm 2 Selective Cache-Efficient Token Processing in iFlame

Require: x_t : Input token at position t
Require: \mathcal{S} : Inference state with cached representations
Ensure: y_t : Output logits for current token

```

1: function PROCESSTOKEN( $x_t$ )
2:    $t \leftarrow \mathcal{S}.\text{position}$ 
3:    $x_t \leftarrow \text{Embed}(x_t)$   $\triangleright$  Token embedding and
      normalization
4:   /* Determine update schedule */
5:    $\phi_0 \leftarrow \text{True}$   $\triangleright$  Update encoder stage 0
6:    $\phi_1 \leftarrow (t + 1) \bmod 3 = 0$   $\triangleright$  Update encoder stage 1
7:    $\phi_b \leftarrow (t + 1) \bmod 9 = 0$   $\triangleright$  Update bottleneck
8:    $\psi_0 \leftarrow (t + 1) \bmod 3 = 0$   $\triangleright$  Update decoder stage 0
9:    $\psi_1 \leftarrow \text{True}$   $\triangleright$  Update decoder stage 1
10:  /* Encoder pathway (downsampling) */
11:  if  $\phi_0$  then
12:     $e_0 \leftarrow \text{EncoderBlock}_0(x_t)$ 
13:     $\mathcal{S}.\text{cache}_E[0][t \bmod 3] \leftarrow e_0$ 
14:  end if
15:  if  $\phi_1$  then
16:     $z \leftarrow \text{Downsample}(\mathcal{S}.\text{cache}_E[0])$ 
17:     $e_1 \leftarrow \text{EncoderBlock}_1(z)$ 
18:     $\mathcal{S}.\text{cache}_E[1][\lfloor t/3 \rfloor \bmod 3] \leftarrow e_1$ 
19:  end if
20:  /* Bottleneck processing */
21:  if  $\phi_b$  then
22:     $z \leftarrow \text{Downsample}(\mathcal{S}.\text{cache}_E[1])$ 
23:     $b \leftarrow \text{BottleneckBlock}(z)$ 
24:     $\mathcal{S}.\text{cache}_D[0] \leftarrow \text{Upsample}(b)$ 
25:  end if
26:  /* Decoder pathway (upsampling) */
27:  if  $\psi_0$  then
28:     $d_0 \leftarrow \mathcal{S}.\text{cache}_D[0]$   $\triangleright$  Retrieve upsampled state
29:     $d_0 \leftarrow d_0 + \mathcal{S}.\text{cache}_E[1]$   $\triangleright$  Skip connection
30:     $d_0 \leftarrow \text{DecoderBlock}_0(d_0)$ 
31:     $\mathcal{S}.\text{cache}_D[1] \leftarrow \text{Upsample}(d_0)$ 
32:  end if
33:  if  $\psi_1$  then
34:     $d_1 \leftarrow \mathcal{S}.\text{cache}_D[1]$   $\triangleright$  Retrieve upsampled state
35:     $d_1 \leftarrow d_1 + \mathcal{S}.\text{cache}_E[0]$   $\triangleright$  Skip connection
36:     $d_1 \leftarrow \text{DecoderBlock}_1(d_1)$ 
37:  end if
38:   $y_t \leftarrow \text{OutputProjection}(d_1)$   $\triangleright$  Project to vocabulary
39:   $\mathcal{S}.\text{position} \leftarrow t + 1$   $\triangleright$  Update position counter
40:  return  $y_t$ 
41: end function

```

Model	MeshGPT[35]	MeshAnyth[4]	MeshAnythv2[5]	MeshXL[3]	PivotMesh[42]	EdgeRunner[38]	BPT[43]	Meshtron[18]	Ours
Unconditional Generation	✓	✗	✗	✓	✓	✗	✗	✗	✓
Attention Networks	Full Plain	Full Plain	Full Plain	Full Plain	Full Plain	Full Plain	Full Plain	Full Hourglass	Interleaving Hourglass
Core Contributions	Autoencoder	Scaling	Sequence Ordering	Scaling	Autoencoder	Autoencoder	Sequence Ordering	Architect	Architect

Table 1. Comparison of different mesh generation models and their key characteristics.

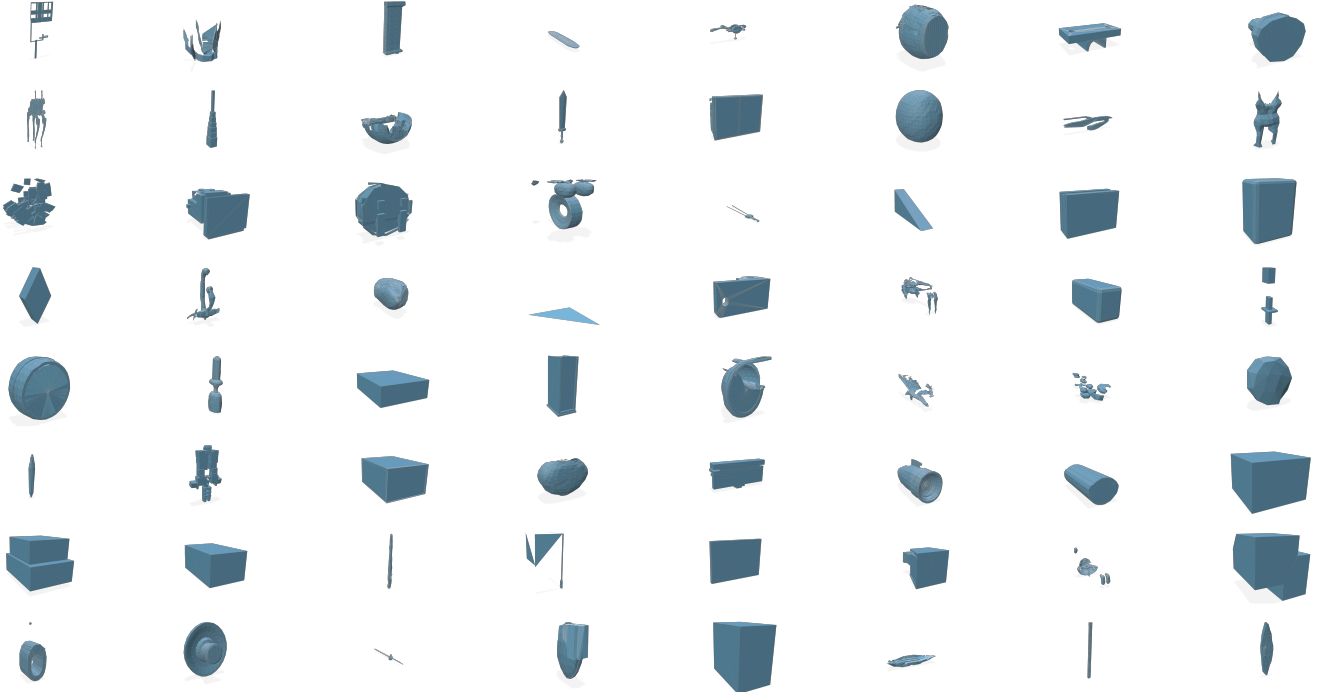


Figure 1. More generative results on Objaverse.

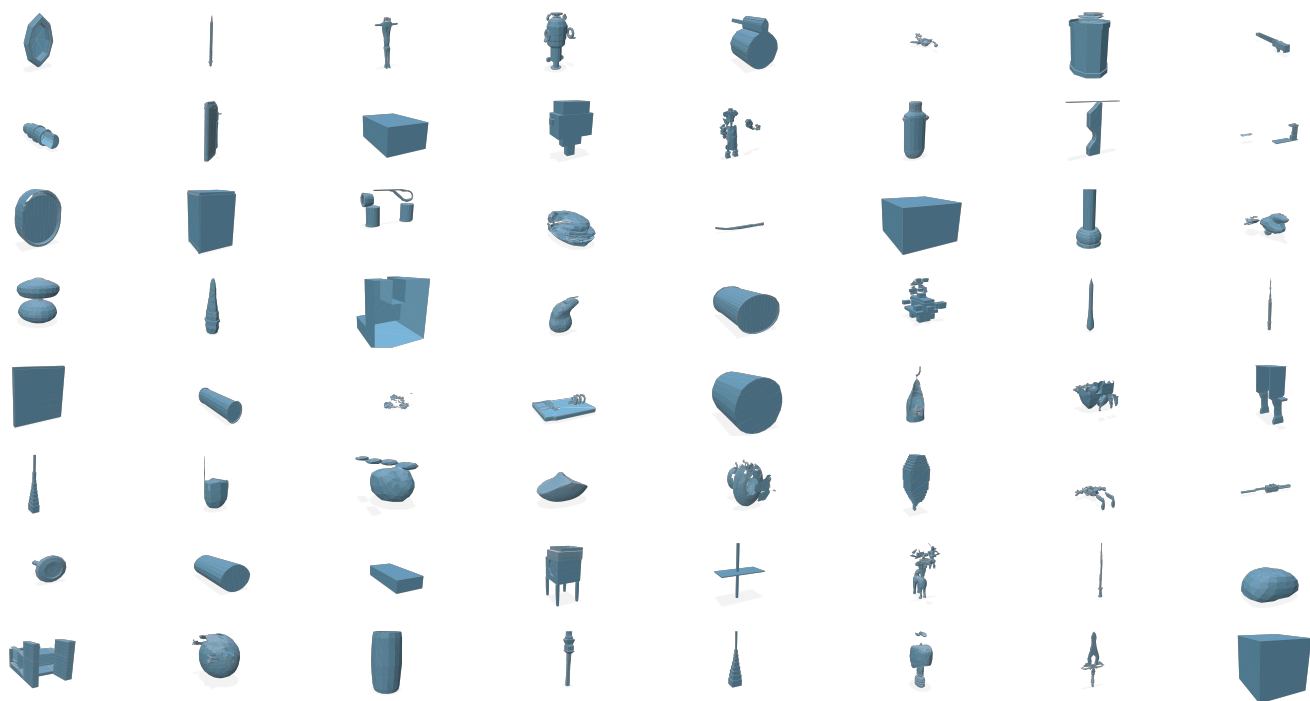


Figure 2. More generative results on Objaverse.

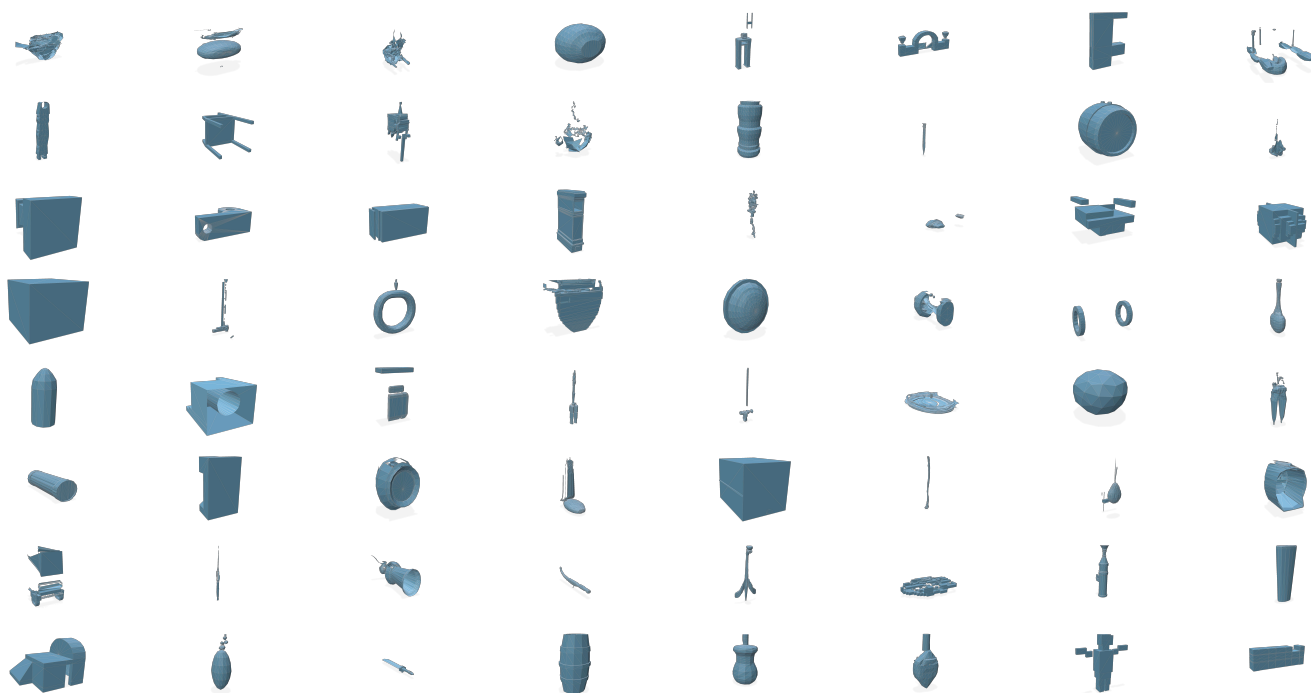


Figure 3. More generative results on Objaverse.